Scripta Materialia 181 (2020) 66–69

Contents lists available at ScienceDirect

Scripta Materialia

journal homepage: www.elsevier.com/locate/scriptamat

Atomic-scale properties of jogs along 1/2⟨110⟩{$\bar{1}$10} edge dislocations in MgO

Jian-Hui Zhai, Pierre Hirel, Philippe Carrez*

Univ. Lille, CNRS, INRA, ENSCL, UMR 8207-UMET-Unité Matériaux et Transformations, F-59000 Lille, France

ARTICLE INFO

Article history:
Received 16 January 2020
Revised 4 February 2020
Accepted 5 February 2020

Keywords:
Binary oxides
Creep
Dislocation
Jog
Modeling

ABSTRACT

We report atomic-scale simulations of the structure and formation energies of jog pairs on 1/2⟨110⟩{$\bar{1}$10} edge dislocations in magnesium oxide (MgO). The atomic configurations of elementary jogs of height 1/4[$\bar{1}$10] and super-jogs of height 1/2[$\bar{1}$10] are fully characterized showing that stable jogs spread in {111}. Besides, our simulations confirm that elementary jogs carry an electric charge $\pm q/2$ where q is the charge of a Mg ion, while super-jogs are charge-neutral. The computation of the formation energy reveals the predominance of charged elementary jogs. This offers new insight into the mechanisms for dislocation climb in MgO.

High-temperature creep of crystalline materials is often associated with the climb of dislocations, a non-conservative process where a dislocation absorbs or emits vacancies [1]. As a dislocation cannot diffuse as a whole line, the interaction with point defects is responsible for the formation of jogs, which become the dominant sources or sinks for vacancies. In turn, the movement of jogs results in the climb of the dislocation. Usual analytical expression of the climb velocity, derived from a continuum description of matter and the classical diffusion theory, are nowadays given in numerous textbooks on dislocation [2]. Usual climb velocity expressions include the effects of the applied stress, temperature and point defect concentration, but disregard the intrinsic properties of jogs [3].

The creep properties of magnesium oxide MgO have been a subject of investigation for some years, as recently reviewed in ref. [4]. Yet the atomistic details of climb are still poorly characterized and early attempts to model jog configurations failed to deliver meaningful energies [5]. More recent studies focused on the interaction of vacancies with screw dislocations or grain boundaries [6,7], yet the properties of jogs on edge dislocations remain unresolved.

Up to now, the questions of jog structure and energetics (formation and migration energies) have been successfully addressed in metals by combining atomistic simulations and kinetic Monte Carlo methods [8–13]. Application to oxides or ceramics is more challenging due to the presence of ions which are electrically charged. In simple oxides with the rock-salt lattice, it has been established since more than a half century that different jog configurations can be anticipated for edge dislocations of 1/2⟨110⟩ Burgers vector [5]. Indeed, a 1/2⟨110⟩{$\bar{1}$10} edge dislocation can climb by the nucleation of three different types of jogs (Fig. 1): elementary jogs (hereafter labeled E^+ or E^-), or super-jogs that can form either an abrupt step (S_I^0) or be formed of two elementary jogs (S_{II}^0). By geometrical considerations on charge balance, Seitz was the first to argue that elementary jogs should carry an electric charge equal to half the charge of an ion while super-jogs are expected to be neutral [14]. The predominance of one type of jogs over the others is however specific to the material's chemical composition. By evaluating the balance between elastic and electrostatic forces, Brækhus and Lothe estimated that neutral super-jogs should dominate in rock-salt chlorates (NaCl, KCl and AgCl), whereas electrically charged elementary jogs should be more common in lithium fluoride LiF [15]. Yet these arguments were based on a geometrical structure of jogs and on a classical estimation of forces, neglecting the effects of atoms relaxation.

In this work, we model at the atomic scale the various types of jogs along a 1/2⟨110⟩{$\bar{1}$10} edge dislocation in MgO. Accounting explicitly for ions charges and relaxations, we quantify the electric charge of jogs, demonstrating that elementary jogs carry an electric charge while super-jogs are charge-neutral. For the first time we precisely compute the formation energies of jog pairs, and demonstrate that dislocation climb occurs through the nucleation of charged elementary jogs.

* Corresponding author.
E-mail address: philippe.carrez@univ-lille.fr (P. Carrez).

https://doi.org/10.1016/j.scriptamat.2020.02.013
1359-6462/

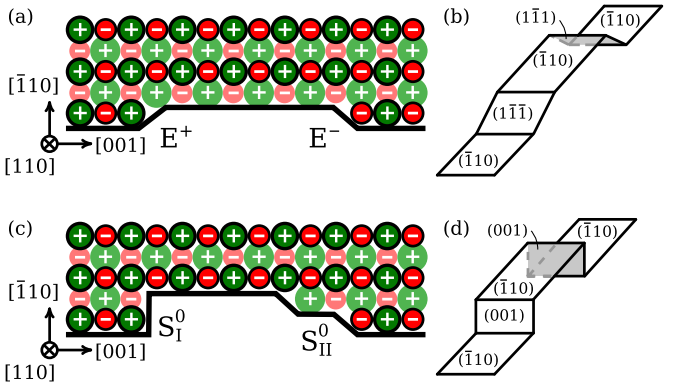

Fig. 1. Schematic picture of jog configurations in a rock-salt lattice. Cations are represented as large green circles, anions as small red circles. Filled black circles represent ions in current plane, and shaded circles those behind the current plane. (a) A pair of elementary jogs, associated with a climb of $1/4[\bar{1}10]$. These jogs climb in {111} planes, as pictured in (b). (c) Two possible configurations for super-jogs: on the left, super-jog forming a right-angle with the initial dislocation (S_I^0), spread in the (001) plane, as pictured in (d). On the right, a super-jog formed of two consecutive elementary jogs (S_{II}^0), which spreads in a {111} plane. (For interpretation of the references to colour in this figure legend, the reader is referred to the web version of this article.)

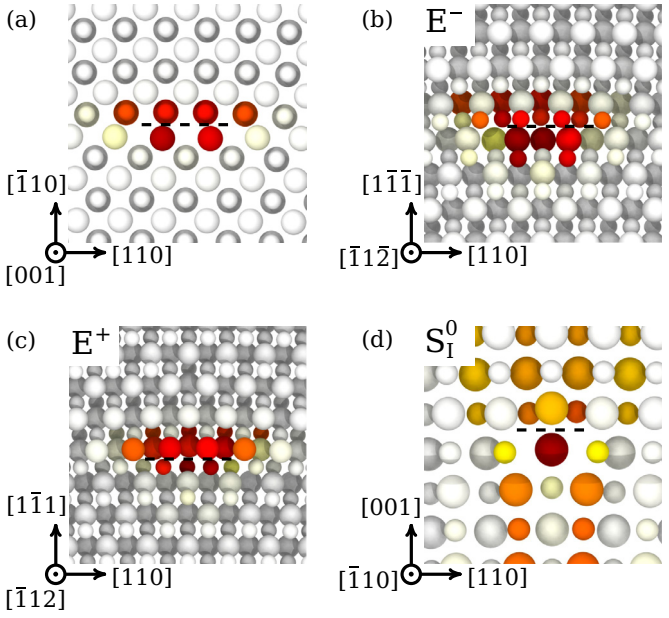

Fig. 2. Atomic configurations of the edge dislocation and jog structures of Burgers vector $\boldsymbol{b} = 1/2[110]$ obtained in this study. (a) The initial dislocation spreads in its $(\bar{1}10)$ glide plane. (b) and (c) are configurations of the elementary jogs (E^- and E^+ respectively) spread in {111} planes. (d) Configuration of the super-jog of type S_I^0 that spreads in the (001) plane. The glide planes are marked as dashed lines. Mg and O ions are represented as large and small spheres respectively, and colored according to their centro-symmetry parameter [19]. Visualization is performed with OVITO [20].

All calculations presented hereafter rely on molecular static simulations performed with the LAMMPS package [16]. Interactions between ions are described with the pair-wise potential parameterization proposed by Henkelman and coworkers [17], which accounts for long-range Coulomb interactions with partial ionic charges of $\pm$ 1.7e (where e is the absolute charge of an electron), and for short-range interactions through a Buckingham function. In all simulations, the Coulomb part is computed by means of the particle-particle particle-mesh (pppm) method [18], and the energy is minimized using a conjugate-gradients algorithm.

The simulated system is a MgO single crystal with the orientation $X = [110]$, $Y = [\bar{1}10]$, $Z = [001]$, containing a dipole of edge dislocations of opposite Burgers vectors $\boldsymbol{b} = \pm 1/2[110]$, such that the simulation is 3-D periodic. Both atoms positions and cell geometry are fully optimized so that the plastic strain due to the dipole vanishes. Fig. 2(a) shows the atomic configuration of a fully relaxed edge dislocation. It should be noted that this dislocation, lying along [001] and terminated by a half-plane of alternating Mg and O ions, is charge neutral.

Jog pairs are then introduced into the system by displacing part of one or two rows of atoms from one dislocation core into the core of the second dislocation. Doing so with a single row of ions, we introduce four elementary jogs of height $1/4[\bar{1}10]$. Displacing two rows of ions generates super-jogs of height $1/2[\bar{1}10]$. If the two displaced rows contains the same number of ions, the resulting super-jogs are of type S_I^0, while if the top row contains fewer ions then super-jogs of type S_{II}^0 are formed. Because the introduction of jogs breaks the symmetry along the dislocation line, the jogged systems are built in such a way that the width of a jog pair is half the simulation cell length $L_z/2$, so that jogs are equally spaced. In order to minimize the cross elastic influence between jogged dislocations, we paid attention to construct systems that all have the same aspect ratio. In the following, all results have been obtained using systems of aspect ratio $L_x \approx L_y \approx 3.5L_z$, corresponding to a number of ions from 50,000 to 4,700,000.

The atomic configurations of the relaxed elementary jogs are reported in Fig. 2. We find that a pair of elementary jogs is composed of two different jogs that spread in {111} planes (as illustrated schematically in Fig 1(b)), but differ in their atomic structure. One jog (E^-) has the structure of an edge dislocation terminated with extra oxygen ions (Fig. 2(b)), while the other (E^+) is terminated with extra Mg ions (Fig. 2(c)). These configurations are thus expected to carry electric charges of opposite signs, just like the edge $1/2\langle 110\rangle\{111\}$ dislocation does in rock-salt structure. This can be verified by evaluating the local charge density in our simulated volume. Following the procedure proposed in Ref. [21], the charge density is evaluated by assigning each relaxed ion a Gaussian function proportional to its electric charge. In defect-free regions, the Gaussians overlap results in vanishing charge density, while in defective regions a net charge density arises due to partially overlapping Gaussians. The resulting charge density for the system containing elementary jogs is reported in Fig. 3(a). By integration of the charge density around each jog, and accounting for the dielectric permittivity of MgO ($\epsilon_r = 8.5$), we obtain an effective charge of 0.85e for the Mg-terminated jog, and $-0.85e$ for the oxygen-terminated one. In other words, elementary jogs carry a charge $\pm\, q/2$ where $q = 1.7e$ is the absolute charge of ions, in agreement with the predictions of Seitz [14].

In contrast, the super-jog S_I^0 forms an angle of 90° with the initial dislocation line, and spreads in the (001) plane as schematically shown in Fig 1(d) and confirmed by the optimized atomistic configuration reported in Fig. 2(d). In this case, a jog pair is formed by two equivalent super-jogs S_I^0 with the structure of a $1/2[110](001)$ edge dislocation segment. This super-jog is terminated by a pair of Mg and O ions, suggesting charge neutrality. By evaluating the corresponding charge density as before, we find that it is weak at super-jogs sites (Fig. 3(b)). Its integration confirms that super-jogs S_I^0 are indeed charge neutral.

Finally, the super-jog S_{II}^0 also allows the dislocation to climb over a lattice vector $1/2[\bar{1}10]$. Such a super-jog is equivalent to stacking two elementary jogs of opposite signs. In a jog pair, one super-jog corresponds to a stacking E^+ on top of E^-, and the other E^- on top of E^+. In both cases, we verify that these super-jogs spread in {111} planes. The evaluation of the charge density confirms the charge neutrality of super-jogs S_{II}^0. However, the charge

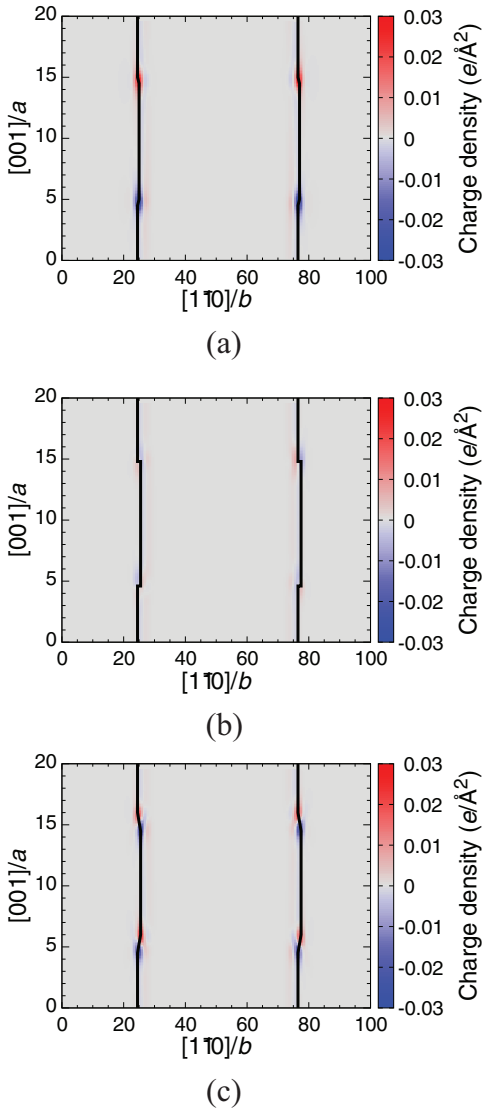

Fig. 3. Charge density of jogs computed from relaxed atomic configurations. Positive charge density appears in red, negative one in blue. The dislocations appear as black lines. Note that each dislocation contains two jogs (one jog pair). (a) Elementary jogs. (b) Super-jogs S_I^0. (c) Super-jogs S_{II}^0. (For interpretation of the references to colour in this figure legend, the reader is referred to the web version of this article.)

density map (Fig. 3(c)) reveals that these super-jogs are associated with an electric dipole moment.

The predominance of one jog type over the others depends on their formation energy H_{jp}^f. Within our frame of work, it corresponds to the difference in energy between the jogged and straight dislocations. Using 3-D periodicity avoids spurious effects usually associated with free or fixed boundary conditions. Nonetheless, long-range interactions exist between jogs and their periodic images, so that the energy difference converges very slowly with the system size (open circles in Fig. 4). These long-range interactions can be of two origins, elastic and electrostatic, noted E_{elast} and E_{elec} respectively. Taking into account that our systems contain two jog pairs, the jog pair formation energy H_{jp}^f is:

$$2H_{jp}^f = (E_{jd} - E_{sd}) - E_{elast} - E_{elec} \quad (1)$$

where E_{sd} is the energy of the system containing straight dislocation lines, and E_{jd} that of the system with jogged dislocations.

Table 1
Properties of jog pairs along 1/2[110]($\bar{1}$10) edge dislocations in MgO. q is the charge of a Mg ion. Energies are given within an uncertainty of 0.02 eV (see text for details).

	height	spreading plane	H_{jp}^f (eV)	charge
pair E^+ E^-	1/4[$\bar{1}$10]	{111}	2.47	$\pm$ q/2
pair S_I^0	1/2[$\bar{1}$10]	(001)	6.02	0
pair S_{II}^0	1/2[$\bar{1}$10]	{111}	4.80	0

For all types of jog pairs, accounting for the periodicity of the system along the dislocation line, the elastic interaction between jogs is given by Lothe [22]:

$$E_{elast} = -4\frac{\alpha h^2}{w}\ln(2) \quad (2)$$

where α is the line tension associated with the bending of the edge dislocation out of its glide plane under applied stress, $w = L_z/2$ the width of the jog pair, and h the jog height. The line tension α is here derived from the prelogarithmic energy factor K for a straight edge dislocation and its second derivative K'' with respect to a small curvature θ out of its glide plane according to the following expression:

$$\alpha(\theta) = \frac{1}{2}\left(K(\theta) + K''(\theta)\right) \quad (3)$$

In the following, K and K'' are calculated within the anisotropic elastic theory as implemented in the BABEL software [23], using a stiffness tensor calculated with the pairwise potential [24], yielding a line tension coefficient $\alpha = 76.03$ GPa · Å^2.

We apply this elastic correction to super-jogs energies as reported with open squares in Fig. 4(a) and (b). In both cases, the resulting jog pair formation energy H_{jp}^f reaches a constant value which is independent of the system size. These values still display small differences of the order of 0.02 eV, which can be attributed to numerical uncertainty, and we take their average as the final formation energy H_{jp}^f. Thus, we find a formation energy of 6.02 eV for a pair of super-jogs S_I^0 and 4.80 eV for super-jogs pair S_{II}^0. Surprisingly, although jogs S_I^0 correspond to dislocation segments of type 1/2⟨110⟩{001}, one of the slip systems of MgO, they have the highest formation energy by far. In contrast, while 1/2⟨110⟩{111} is known to be an unfavorable slip system in MgO, jogs S_{II}^0 spread in {111} have a lower formation energy and thus are the most favorable super-jogs.

In case of elementary jogs, the elastic correction does not allow to recover a system size independent formation energy, as shown in Fig. 4(c). Indeed, as elementary jogs are charged, their electrostatic interaction E_{elec} has to be evaluated and accounted for. We assume this contribution to be a classical summation of Coulomb interaction for an array of point charges $q/2 = \pm 0.85e$ in a medium of dielectric constant ϵ_r. For consistency, this contribution is computed by means of the pppm method. Interestingly, the Coulomb correction has the same order of magnitude as the elastic correction, indicating that both interactions are seemingly important. Finally, averaging of corrected values yields a jog pair formation energy $H_{jp}^f = 2.47$ eV. It should be noted that because elementary jogs have different atomic structures as explained above, our methodology does not allow to distinguish the contributions of individual jogs E^+ and E^-.

The properties of jogs obtained in the present study are summarized in Table 1. The elementary jog pair has the lowest formation energy, so we expect it to be the first event to occur

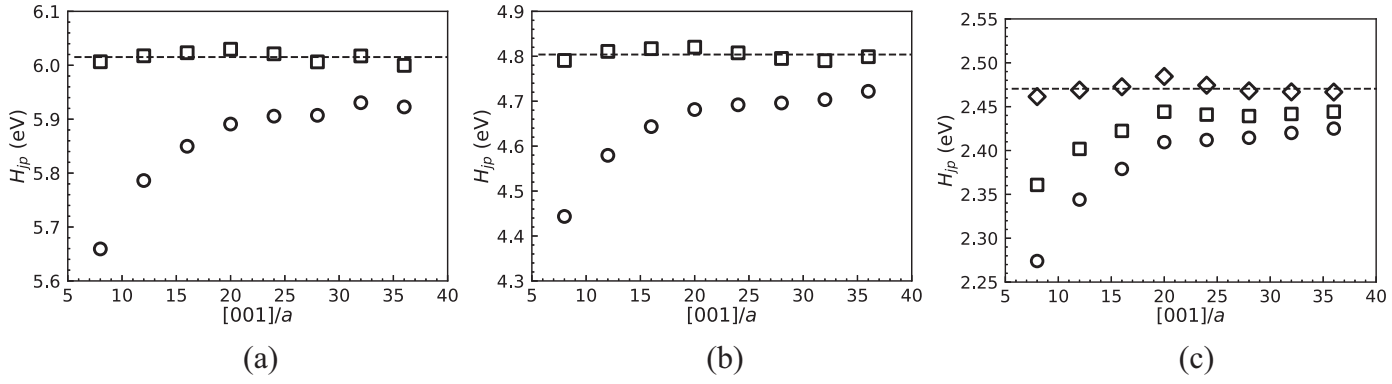

Fig. 4. Jog pair energy as a function of the simulation cell length along $Z = [001]$. (a) Pair of super-jogs S_I^0. (b) Pair of super-jogs S_{II}^0. (c) pair of elementary jogs E^+ and E^-. The value from atomistic simulations is given as open circles, elastic corrected data is given in squares, and fully corrected data (elastic and electrostatic) in diamonds. The dashed line gives the final averaged value H_{jp}^f for the fully corrected data.

when a straight dislocation absorbs point defects, resulting in the climb of a dislocation segment by $1/4[\bar{1}10]$. However, climbing over a lattice vector $1/2[\bar{1}10]$ requires either two consecutive climb stages involving only elementary jogs, or the formation of super-jogs. Since the formation energy for super-jogs S_{II}^0 is comparable to twice that of an elementary jog pair, we expect a competition between those two mechanisms.

Since a stable super-jog S_{II}^0 corresponds to the stacking of two elementary jogs, climb ultimately involves the formation of charged defects. Here, the net charge of jogs naturally arises from the rigid ion potential unable to account for any local relaxation of the electronic structure. The charge of jogs is geometrically related to the core of the edge dislocation in {111}. To check against potential artifacts, we performed additional first principles calculations on a dipole of $1/2\langle 110\rangle\{111\}$ perfect edge dislocations. In these calculations, as for those in Ref. [24], we used the VASP code [25,26] with the PW91 functional and the projector augmented wave method [26] on a cell containing 456 atoms. After a complete relaxation of the electronic structure, we performed a Bader analysis [27] to estimate the charge of each atom. According to the Bader charge decomposition, we verified that charge transferred in the vicinity of the dislocation cores is identical to that occurring in bulk MgO. As a result, the dislocation that contains an excess of Mg atoms is positively charged, and the other is negatively charged, giving us confidence in the charge $\pm q/2$ carried by jogs in this study.

Similarly as in metals, jogs impose an elastic interaction on point defects, in particular vacancies. The difference in MgO is that vacancies as well as elementary jogs carry an electric charge, resulting in an additional interaction which can be attractive or repulsive depending on the sign of their respective charges. The charge carried by elementary jogs being half that of an ion charge, it cannot be neutralized by emission or absorption of intrinsic point defects. Indeed, a jog E^+ attracting a cationic vacancy turns into a jog E^-. Absorption or emission of vacancies results not only in the migration of the jog, but also in the inversion of its charge. Therefore, jog point defects interaction should be considered explicitly when modeling dislocation climb, in atomic-scale simulations as well as in coarse-grained models. Our findings can be directly applied to upper scale modeling of creep such as kinetic Monte Carlo or dislocation dynamics, at the condition that it implements electrostatic interaction between jogs and point defects, and can reproduce the change of charge of jogs when it absorbs or emits defects. We also hope that the methodology laid out in this study can be used to study dislocation jogs and climb in other materials.

Declaration of Competing Interest

The authors declare that they have no known competing financial interests or personal relationships that could have appeared to influence the work reported in this paper.

Acknowledgements

This study was supported by the French government through the Programme Investissement d'Avenir (I-SITE ULNE / ANR-16-IDEX-0004 ULNE) managed by the Agence Nationale de la Recherche, under the project name LASCO. Computational resources have been provided by the CRI at Université de Lille. We warmly acknowledge fruitful discussions with Emmanuel Clouet from CEA Saclay, France.

References

[1] J.P. Hirth, J. Lothe, Theory of Dislocations, Krieger Publishing Company, 1982.
[2] D. Caillard, J.-L. Martin, Thermally Activated Mechanisms in Crystal Plasticity, 8, Elsevier, 2003.
[3] E. Clouet, Phys. Rev. B 84 (9) (2011) 092106.
[4] J. Amodeo, S. Merkel, C. Tromas, P. Carrez, S. Korte-Kerzel, P. Cordier, J. Chevalier, Crystals 8 (6) (2018) 240.
[5] R.W. Whitworth, Adv. Phys. 24 (2) (1975) 203–304.
[6] K. Kolluri, E. Martinez Saez, B.P. Uberuaga, Chem. Mater. 30 (6) (2018) 1980–1988.
[7] X. Liu, E. Martinez, B.P. Uberuaga, Sci. Rep. 9 (2019) 6499.
[8] D. Rodney, R. Phillips, Phys. Rev. Lett. 82 (8) (1999) 1704–1707.
[9] B. Wirth, G. Odette, D. Maroudas, G. Lucas, J. Nucl. Mater. 276 (1) (2000) 33–40.
[10] T. Vegge, K.W. Jacobsen, J. Phys.: Condens. Matter 14 (11) (2002) 2929–2956.
[11] T.T. Lau, X. Lin, S. Yip, K.J.V. Vliet, Scr. Mater. 60 (6) (2009) 399–402.
[12] M. Kabir, T.T. Lau, D. Rodney, S. Yip, K.J. Van Vliet, Phys. Rev. Lett. 105 (2010) 095501.
[13] M. Landeiro Dos Reis, L. Proville, M. Sauzay, Phys. Rev. Mater. 2 (2018) 093604.
[14] F. Seitz, Phys. Rev. 79 (1950) 890–891.
[15] J. Braekhus, J. Lothe, Physica Status Solidi (b) 51 (1972) 149–153.
[16] S. Plimpton, J. Comput. Phys. 117 (1) (1995) 1–19.
[17] G. Henkelman, B.P. Uberuaga, D.J. Harris, J.H. Harding, N.L. Allan, Phys. Rev. B 72 (11) (2005) 115437.
[18] M.P. Allen, D.J. Tildesley, Computer Simulation of Liquids, 2nd, Oxford University Press, 2017.
[19] C.L. Kelchner, S. Plimpton, J. Hamilton, Phys. Rev. B 58 (17) (1998) 11085.
[20] A. Stukowski, Model. Simul. Mater. Sci. Eng. 18 (1) (2009) 015012.
[21] P. Hirel, P. Carrez, E. Clouet, P. Cordier, Acta Mater. 106 (2016) 313–321.
[22] J. Lothe, in: Modern Problems in Condensed Matter Sciences, 31, Elsevier, 1992, pp. 175–235.
[23] E. Clouet, Babel software, (http://emmanuel.clouet.free.fr/Programs/Babel/index.html).
[24] P. Carrez, D. Ferré, P. Cordier, Modell. Simul. Mater. Sci. Eng. 17 (3) (2009) 035010.
[25] G. Kresse, J. Furthmüller, Comput. Mater. Sci. 6 (1) (1996) 15–50.
[26] G. Kresse, D. Joubert, Phys. Rev. B 59 (3) (1999) 1758.
[27] G. Henkelman, A. Arnaldsson, H. Jnsson, Comput. Mater. Sci. 36 (3) (2006) 354–360.